

Research Article

Comparative Surface Interaction Study to Detect *Brucella melitensis* 16M Using Biosensor Transducer Modifications with 4-MBA, ZnONPs/AuNPs, ZnONPs/AuNPs/4-MBA

Hans R¹; Thavaselvam D^{2*}

¹Division of Biodetector Development Test and Evaluation, Defence Research and Development Establishment, Defence Research and Development Organisation, India

²Director (PM) O/o Director General Life Sciences (DGLS), Defence Research and Development Organization (DRDO) Headquarters, Ministry of Defence, SSPL Campus, India

***Corresponding author: Thavaselvam D**

Director (PM) O/o Director General Life Sciences (DGLS), Defence Research and Development Organization (DRDO) Headquarters, Ministry of Defence, SSPL Campus, India.

Received: December 09, 2022

Accepted: January 30, 2023

Published: February 06, 2023

Abstract

Brucellosis is a zoonotic disease endemic in developing countries and caused by gram-negative bacteria of genus *Brucella* infecting both livestock and humans. *Brucella melitensis* and *Brucella abortus* are important species representing largest biotypes world-wide. Therefore, modified detection strategies and advancement in potential analytical tools are required to monitor its rapid prevalence. In this study, we aim to modify gold-transducer of Surface Plasmon Resonance biosensor with combination of metal oxide nanomaterials and chemical probe to detect recombinant outer membrane 'rOmp28' protein antigen of *Brucella melitensis* 16M in concentration-dependent surface interactions. We synthesized Zinc (ZnONPs) and Gold (AuNPs) nanoparticles using standard 'Hydrothermal and Turkevich Methods' and their crystalline structure, chemical property and morphology were analysed using UV-Visible Spectrophotometry, FT-IR, Powder-XRD, SEM-EDX and TEM-SAED. For immobilizing specific rOmp28 derived IgG-pAbs on modified Au-transducer, rOmp28 protein was expressed and purified using Ni-NTA gel affinity chromatography for producing pAbs in BALB/c mice. Three modifications of Au-transducer with 4-MBA, ZnONPs/AuNPs and ZnONPs/AuNPs/4-MBA were subjected for immobilization and SPR biosensing was performed with rOmp28 Ag at detection range of 0.1 $\mu\text{g mL}^{-1}$ to 0.01 fg mL^{-1} . Limit of detection observed with ZnONPs/AuNPs/4-MBA combination was 0.1 fg mL^{-1} by relative increase in SPR response angle at 0.1 $\mu\text{g mL}^{-1}$ in the order 83.7° < 98.9° < 179.2° for 4-MBA < ZnONPs/AuNPs < ZnONPs/AuNPs/4-MBA respectively. In conclusion, metal oxide nanomaterials in combination with biosensor are suitable in sensitive and specific interaction of antigen displaying lowest LODs and enhanced biosensor response for on-field real-time *Brucella* detection in both clinical and non-clinical disease scenario.

Keywords: *Brucella*; Recombinant Protein rOmp28; Zinc Nanoparticles; Gold Nanoparticles; Surface Plasmon Resonance; Biosensors

Abbreviations: rOmp28: Recombinant Outer Membrane Protein; OMP: Outer Membrane Protein; Bm16M: *Brucella melitensis* 16M Strain; *E coli*: *Escherichia coli*; Ag: Antigen; Ab or pAb: Polyclonal Antibody; LPS: Lipopolysaccharide; SPR: Surface Plasmon Resonance, Au-transducer Gold Transducer; NCTC: National Collection of Type Cultures; PHE: Public Health England; Biosafety Level; HCF: High Containment Facility; LAIs: Laboratory Acquired Infections; LOD: Limit of Detection; IgG: Immunoglobulins G; IgM: Immunoglobulin M; SAT: Serum Agglutination Test; MCDA: Multiple Cross Displacement Isothermal Amplification; PCR: Polymerase Chain Reaction;

rtPCR: Real-Time Polymerase Chain Reaction; ELISA: Enzyme Linked Immunosorbent Assay; I-ELISA: Indirect-Enzyme Linked Immunosorbent Assay; CFU: Colony Forming Units; BSA: Bovine Serum Albumin; BSB: *Brucella* Selective Broth; LB: Luria Bertani Broth; BHI: Brain Heart Infusion Broth; IPTG: Isopropyl β -D-1-thiogalactopyranoside; CFA: Complete Freund's Adjuvant; IFA: Incomplete Freund's Adjuvant; HIS: Hyper Immune Sera; PIS: Pre-Immune Sera; EDC N-(3-Dimethylaminopropyl)-N'-ethylcarbodiimide Hydrochloride; NHS: N-Hydroxysuccinimide; 4-MBA 4-Methoxybenzoic Acid; SAMs: Self-Assembled Monolayers; NPs: Nanoparticles; ZnO: Zinc Oxide; ZnONPs: Zinc Oxide Nanoparticles; AuNPs Gold Nanoparticles; UV: Vis Ultra-Violet Visible; FT-IR: Fourier Transform Infra-Red Spectroscopy; XRD: X-ray Powder Diffraction; SEM-EDX: Scanning Electron Microscopy with Energy Dispersive X-ray Analysis, TEM-SAED: Transmission Electron Microscopy with Selected Area Diffraction; fcc: Face Centered Cubic; Ni-NTA: Nickel Nitriloacetic Acid; SDS-PAGE: Sodium Dodecyl Sulfate - Polyacrylamide Gel Electrophoresis; kDa: Kilo Daltons; kV: Kilovolts; DI: De-ionized Water; RT: Room Temperature; pH: Potential of Hydrogen Ion; 2θ Theta Angle; PBS: Phosphate Buffered Saline; PBS-T: Phosphate Buffered Saline with Tween-20; O/N: Overnight; IAEC: Institutional Animal Ethics Committee; IBSC: Institutional Biosafety Committee; CIF: Central Instrumentation Facility.

Introduction

Brucella is a causal agent of the disease brucellosis and its prevention and control in endemic areas is most relevant in concern to both animal and human health. To eradicate its rapid re-occurrence and frequent spread, there is an urgent need to control animal infections and its concurrent passage to humans [1]. It is a zoonotic infection of medical importance and animals are the principal seedbeds for disease interplay between animal to animal and animal to human successive transmissions [2]. The bacteria belong to genus *Brucella* and most common species prevalent in livestock infection are *Brucella abortus* and *Brucella melitensis* [3,4]. Infection in human was reported by four major species of *Brucella* basically, *Brucella melitensis* (from camels, sheep or goats), *Brucella suis* (pigs), *Brucella abortus* (cattle) and *Brucella canis* (dogs), in descending order of pathogenicity [5]. Although, despite of its endemicity in developing countries, many of the developed nations have strategically control the spread of brucellosis but in past 3 years it has been reported as a most re-current, re-emerging, intermittent infection in Japan, China, India, Australia and other European Countries [6]. Progressive risk of contamination occurs with close contact to infected animals or through generated aerosols, continuous bacterial shedding by underlying tissues, raw under-cooked meat, food articles of animal origin and spontaneously through incomplete processing of milk and its by-products [7]. Disease symptoms of typical flu-like allergy begins with acute illness and later on progresses with neurological involvement of central and peripheral system in chronic derivatives [8]. The delayed diagnosis and early treatment bias happens due to in-sufficient knowledge by physicians, disease under-diagnosis, bacterial mis-identification by related differential diseases and low index of disease speculation among urban population has contributed to the widespread of brucellosis with in-sufficient case-reports [9]. Due to the risk factors associated with human health and community transmission at large scale, it is ranked as 'bio-pathogen of concern' to be handled carefully in bio safety levels (BSL-3 laboratories) in order to prevent LAIs, laboratory acquired infections [10]. In global scenario, brucellosis is reported among the top ten zoonosis of concern with highest impact

on human health and agro-economy. It is gradually emerging and re-emerging in more than 170 countries across six major regions of the globe with approximately, 500,000 new human infections reported annually along with persisted endemic cases worldwide [11]. Clinically, brucellosis is often mis-diagnosed with other febrile illness viz; Typhoid and Malaria, representing non-distinct acute or sub-acute infection but with the disease progression, its chronic illness likely projects more severe symptoms and focal complications. Therefore, for its proper diagnosis and early management of acute and chronic fevers a detailed occupational or travel history of the patient must be critically entertained [12]. Gold standard established for *Brucella* detection is using blood cultures but they generally present variable sensitivity and needs minimum 30 to 40 days for culture based typing and sub-culturing for further analysis based upon biochemical, molecular and immunological methods [13]. Other methods for diagnosis and rapid testing employs antibody agglutination assays like Serum Agglutination Test (SAT) but it mostly lacks agglutination at higher antibody titers and results in false negative interpretation due to high prozone effects [14,15]. Serological tests like Rose Bengal Agglutination Test, Direct and Indirect Fluorescent Polarization Antibody Test, Complement Fixation Test, 2- β Mercaptoethanol, Indirect Coomb's Test, Brucellacapt, Dipstick, Micro agglutination and Dot Blot Assays are often used for its rapid detection [16,17]. But, they are also known to present false positive results due to non-specific and non-agglutinating 'blocking antibodies' in severe chronic infection [18,19]. Enzyme immunoassay like ELISAs and Lateral Flow assays are more sensitive and often used as choice-of-tests but they also lack detection at lower antibody titers and are unable to distinguish between acute and chronic infections with IgG and IgM antibodies distinctly [20,21]. In addition, an enzyme-labelled antibody is needed for both direct and indirect ELISAs along with long experimental procedures [22]. On contrary, molecular tests like PCR, rtPCR and other fluorescence and probe based quantitative PCRs, Isothermal and Polymerase Amplifications are sensitively specific but are difficult to employ commercially in low-resource settings, requires

efficient subject-expertise for pre-sample preparations along with critical analysis of methods and often fails to report on-field pre-clinical acute cases [23]. Therefore, for accurate and confirmed diagnosis, serological, molecular and microbiological techniques are used simultaneously ‘in combination’ to overcome the on-specific and atypical detection of *Brucella* [24]. Since, the existing methods of diagnosis are lengthy, not cost-effective, presents limited specificity, false positive, cross-reactive in differential disease cases, non-suitable for on-field testing, brings variable sensitivity among disease reservoirs etc. Thus, along with combinatorial detection methods, a new approach by introducing metal oxides with assay hybridization, in bio-molecular bio-conjugations using surface modification of bio-sensors can be deciphered for direct real-time on-field *Brucella* biomarker based detection [25,26]. One such novel method is invaluable for rapid and easy detection whereby, lateral flow nanobiosensors which are suitable for on-site miniaturized detections are used to detect *Brucella* employing MCDA, multiple cross displacement isothermal amplification [27]. And, a newly designed colorimetric immunoassay using silica nanoparticles for synthesizing fabricated immunosensors was used in conjunction with selective polyclonal antibody (pAb) against *Brucella abortus* (LOD of 450 CFU mL⁻¹) for on-site rapid detection [28]. Another finding was also reported where label-free impedance immunosensor having fabricated pAbs of *Brucella melitensis* on the surface of gold nanoparticle modified screen-printed carbon electrodes was used to specifically detect *Brucella* whole cells at LOD of 4X10⁵ CFU mL⁻¹ [29]. Therefore, such modified bio-sensors using nanomaterials are proven efficient tools to identify and characterize bacterial pathogens offering real-time detection which is comparatively sensitive and specific with lower limits of pathogen detection. Metal zinc oxide nanoparticles

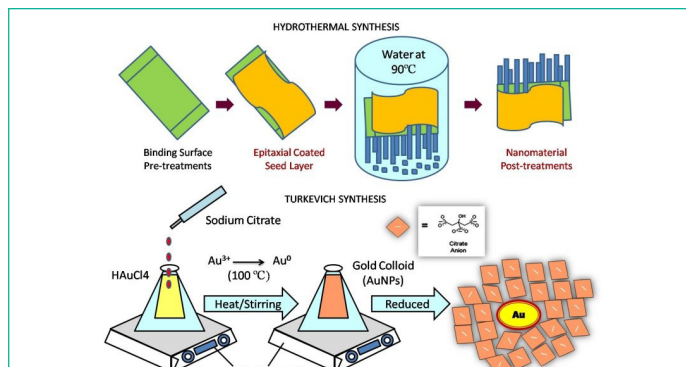


Figure 1: Schematic representation of methodology used in ZnONPs and AuNPs preparation for SPR bio-sensing with Hydrothermal and Turkevich standard methods of nano-synthesis.

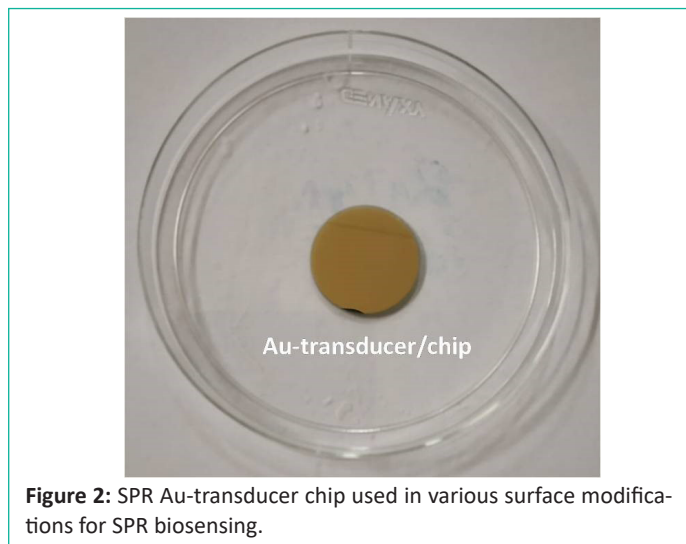


Figure 2: SPR Au-transducer chip used in various surface modifications for SPR biosensing.

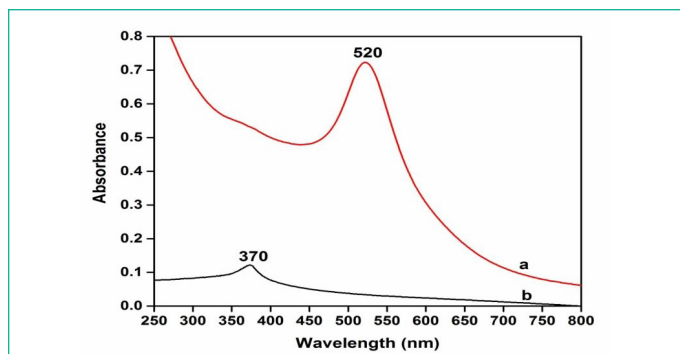


Figure 3: UV-Visible analysis showing absorption spectra of (a) AuNPs (b) ZnONPs with corresponding absorption spectrum peaks at λ_{max} 520nm and λ_{max} 370nm respectively.

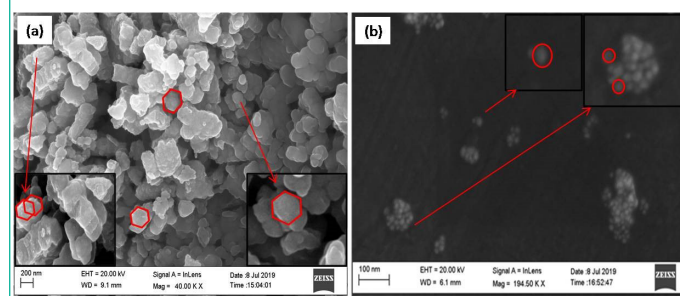


Figure 4: Characterization of ZnONPs and AuNPs with SEM-EDX is showing (a) ZnONPs with ‘Hexagonal Wurtzite’ nano-beads at 200nm (b) AuNPs with ‘Round-Bead and Spherical’ shape nanoparticles respectively.

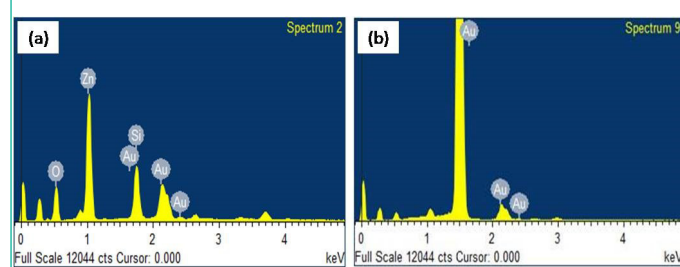


Figure 5: SEM-EDX analysis for (a) ZnONPs with anisotropic growth patterns showing four iterations having O, Si, Zn and Au elements. Elements Au and Si corresponds to Au-transducer elemental composition having ZnO nanoparticles (b) AuNPS showing pure gold elemental iterations with spherical shaped particles having uniform identical patterns.

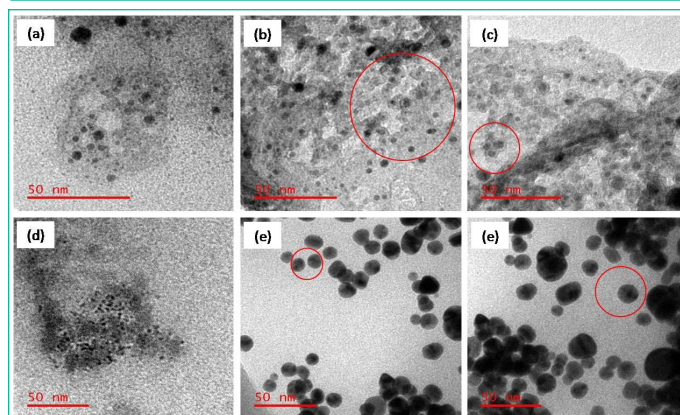


Figure 6: Characterization of ZnONPs and AuNPs with TEM-SAED showing (a, b and c) area under circle for ZnONPs with clearly visible ‘Hexagonal Wurtzites’ particles and, (d, e and f) ‘Spherical Round’ single suspended nano-size structures for AuNPs.

functionalized with selective antibody of *Brucella abortus* for active deposition on metal aluminium sheets has been reported for cyclic voltametric detection of *Brucella* [30]. And, integration of such ZnO metal oxide combined with its hybrid

nanostructures is also reported as efficient in developing potential biomedical sensor devices with unique fabrications to provide accurate and real-time point-of-scale biosensing for selective and sensitive detection [31,32]. Therefore, in our present study, we immobilized highly specific and sensitive IgG-pAbs derived from recombinant outer membrane marker protein antigen (rOmp28 Ag) of *Brucella melitensis* 16M on the modified surface of SPR Au-transducer having three different combinations of selective metal oxide nanomaterials (ZnONPs and AuNPs) along with 4-MBA Self Assembled Monolayered (SAMs) probe molecule. During SPR interaction study with modified biosensor gold chips, *Brucella* rOmp28 antigen was detected at 0.1 fg mL^{-1} as the lowest limit of detection. And, order of sensitivity for antigen detection with increased SPR response angle was observed with ZnONPs/AuNPs/4-MBA modification among the other layered combinations. In conclusion, enhanced modification of SPR Au-transducer using combination of metal oxide nanomaterials is promising in specific detection of *Brucella melitensis* 16M surface protein antigen at lowest detection limit in femtograms. Hence, the selective biosensor modification can be used to deploy in on-field *Brucella* detection for early acute and sub-acute clinical cases with low-antigen availability. This

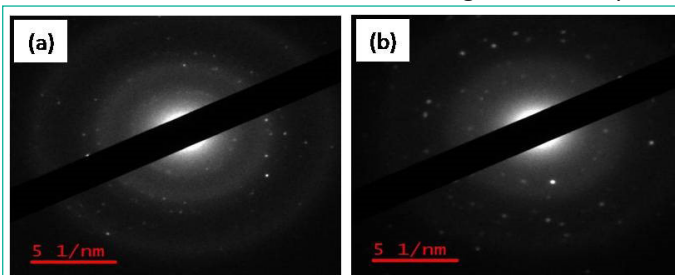


Figure 7: TEM-SAED patterns for (a) ZnONPs in particle size range between 100nm to 200nm with SAED patterns showing bright sharp spots on concentric rings indicating polycrystalline nature of ZnONPs and, (b) AuNPs as round size nano structures having particle size range of between 50 to 100nm with SAED patterns of concentric bright spots corresponding to polycrystalline nature of Au particles.

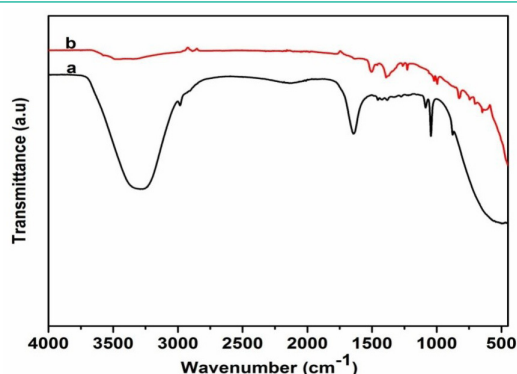


Figure 8: Characterization with FT-IR analysis using wave number range of $4,000\text{cm}^{-1}$ to 500cm^{-1} indicating (a) absorption at $3,400$ to $3,300\text{cm}^{-1}$ for medium N-H stretching vibrations of hydrogen bonds in amines and of pendant hydroxyl groups, peaks at $3,300$ to $2,500\text{cm}^{-1}$ and $1,640$ to $1,403\text{cm}^{-1}$ corresponds to O-H stretching of carboxylic and S-H, C-O stretchings and O-H bending vibration of thiol groups, C=O stretching vibrations of amides and pendant carboxylic groups and frequency peaks at $1,505\text{cm}^{-1}$, $1,382\text{cm}^{-1}$, $1,085\text{cm}^{-1}$, $1,044\text{cm}^{-1}$ corresponds to stretching vibrations of N-O for nitro group and C-H bending and C-O stretching of alkanes and alcohols respectively of AuNPs and, (b) absorption at $3,500$ to $3,450\text{cm}^{-1}$ of strong N-H stretching vibrations of primary amines and medium O-H stretchings, peaks at $1,550$ to $1,500\text{cm}^{-1}$ for N-O stretchings of nitro functional group and peaks at $1,342$ to $1,266\text{cm}^{-1}$, $1,250$ to $1,020\text{cm}^{-1}$ and $1,395$ to $1,310\text{cm}^{-1}$ for C-N stretching vibration of amines, aromatic amines along with O-H bending vibrations of carboxylic groups for ZnONPs.

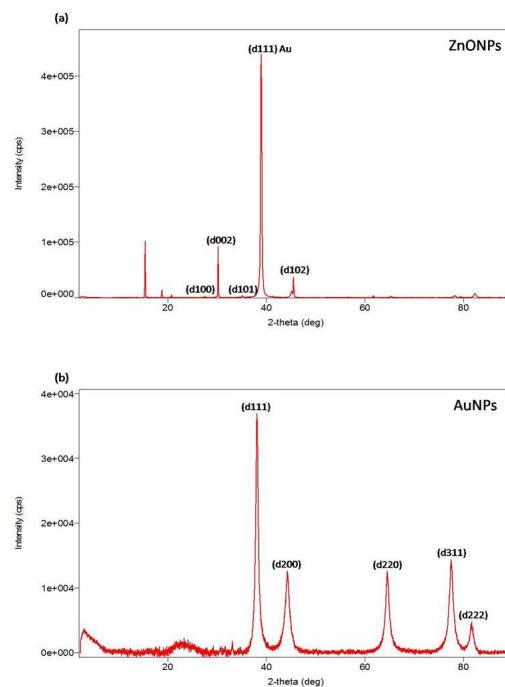


Figure 9: Characterization with powder-XRD analysis indicating (a) d-spacing planes in fcc cubic system for ZnONPs with diffraction peaks with 2θ values at 31.84° , 34.52° , 36.33° and 47.63° for corresponding reflections of (100), (002), (101) and (102) set of planes and, (b) for AuNPs peaks were observed with 2 values at 38.16° , 44.31° , 64.41° and 77.50° for corresponding reflections of (111), (200), (220) and (311) set of planes respectively.

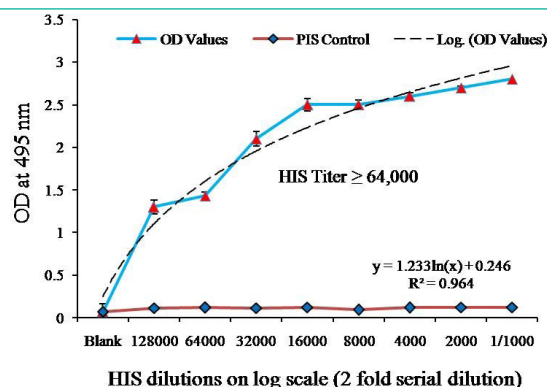


Figure 10: Standard graph plot showing antibody titer estimated using I-ELISA for the developed mice IgG-pAbs against rOmp28 Ag of *Brucella melitensis* 16M. The two fold serial dilutions of HIS resulted in logarithmic regression co-efficient value, $R^2=0.964$ with observed linearity in standard equation $y=1.233\ln(x)+0.246$ in comparison with PIS negative control (1:1000 dilution).

modified approach is simple, reliable, fast and accurate offering selective sensitivity and specificity for antibody mediated surface antigen based detection of *Brucella* to distinguish differential disease pool for clinical diagnosis in low-resource settings.

Materials and Methods

The present study is representing step-by-step preparation and characterization of metal oxide nanomaterials for modification of the SPR Au-transducer chips with various combination of deposited Zn and Au nanomaterials along with well-known probe molecule 4-MBA as shown in schematics (Figure 1 and 15). When 4-MBA was coated on the biosensor chip surface, it resulted in Self Assembled Monolayers (SAMs) having thiol and carboxylic groups for amide linking with EDC/NHS and antibody peptides. Prior to immobilization on modified SPR sensor surface, we have expressed and purified specific recombinant

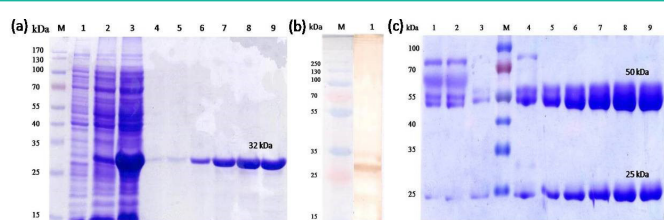


Figure 11: One-dimension SDS-PAGE gel electrophoresis and Immunoblot analysis of rOmp28 protein Ag and its corresponding IgG-pAbs showing (a) expressed and purified 32 kDa molecular size recombinant rOmp28 protein of *Brucella melitensis* 16M with Un-induced (*Escherichia coli* BL-21 bacterial culture) cell lysate (Lane 1), Column Flow Through (Lane 2), 1mM IPTG induced (BL-21 positive culture) clone (Lane 3), purified rOmp28 protein elutes 1 to 6 (Lane 4 to 9) in 8M Urea at denaturing conditions, Lane M with Fermentas #SM0671 protein marker respectively, (b) Immunoblot analysis with specific immuno-reactivity of rOmp28 derived mice IgG-pAbs showing positive immunoblot with characteristic rOmp28 protein antigen (Lane 1) and Lane M with Fermentas #SM1811 protein marker respectively, (c) SDS-PAGE analysis of purified rOmp28 mice IgG-pAbs with affinity column purification showing crude polyclonal HIS (Lane 1 and 2), column wash (Lane 3), flow through (Lane 4), purified mice IgG-pAbs with heavy (50 kDa) and light (25 kDa) chain fragments from elutes 1 to 5 (Lane 5 to 9) and Lane M with Fermentas #SM0671 protein marker respectively.

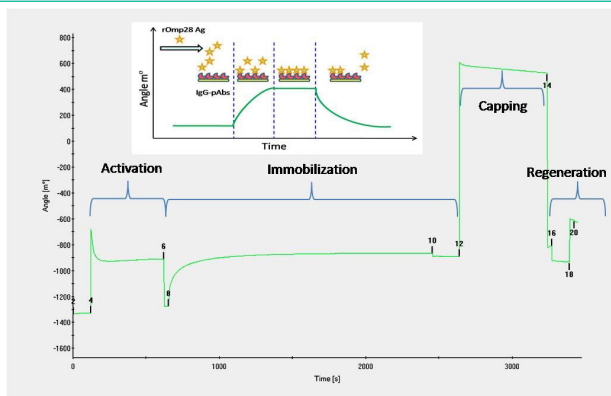


Figure 12: Immobilization of rOmp28 mice IgG pAbs on SPR-Au transducer surface with sensogram showing different steps (Surface Activation with EDC/NHS, Immobilization of ligand IgG-pAbs, Capping with Ethanolamine, Baseline Regeneration with HCl) involved in the biosensing process at time scale(s) on x-axis and SPR response angle (m^2) on y-axis respectively. And, embedded window schematics for surface interaction where m^2 changes on analyte (rOmp28) interaction with ligand (rOmp28 IgG-pAbs) at association, complete saturation occupying all ligands, dissociation from ligand substrate and at the end showing baseline regeneration.

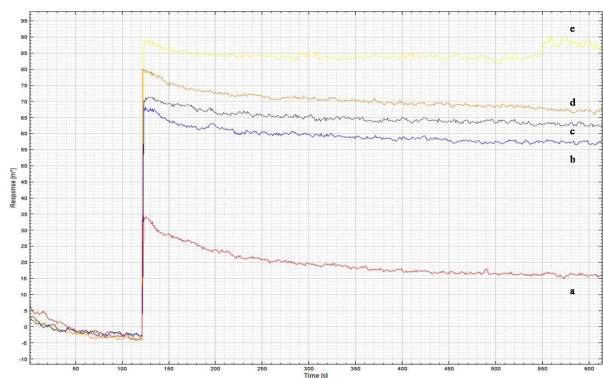


Figure 13: Sensogram showing optimization of SPR sensor response for interaction of test analyte (*Brucella* rOmp28 Ag) with ligand (rOmp28 IgG-pAbs) at 10 fold serial dilution of Ag on Au-transducer surface modified with only ZnONPs (a) PBS buffer (b) $1\mu g mL^{-1}$ (c) $0.01ng mL^{-1}$ (d) $0.1ng mL^{-1}$ (e) $1ng mL^{-1}$ respectively.

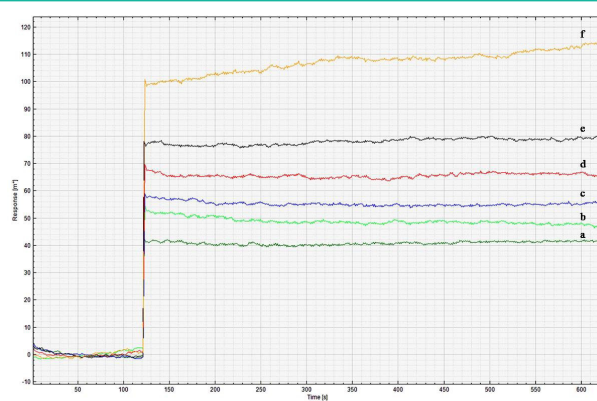


Figure 14: Sensogram showing optimization of SPR sensor response for interaction of test analyte (*Brucella* rOmp28Ag) with ligand (rOmp28 IgG-pAbs) at 10 fold serial dilution of Ag on Au-transducer surface modified with metal oxides nanoparticles ZnONPs/AuNPs (a) PBS buffer (b) $0.1\mu g mL^{-1}$ (c) $0.01\mu g mL^{-1}$ (d) $0.01ng mL^{-1}$ (e) $0.1ng mL^{-1}$ (f) $0.1\mu g mL^{-1}$ respectively.

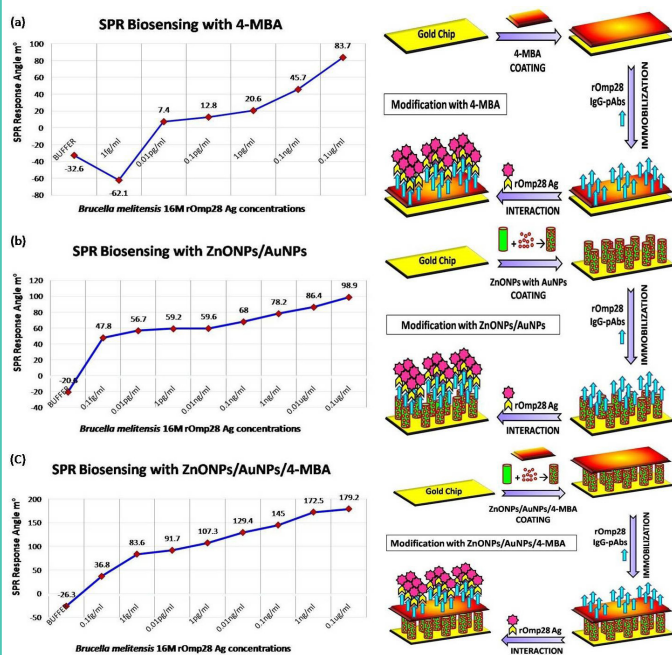


Figure 15: Standard graph plots for surface interaction binding study showing SPR response angle with different Au-transducer modifications and their schematic flow-diagram presenting (a, b and c) interaction of rOmp28 IgG-pAbs as ligand detection antibody with surface analyte rOmp28 antigen of *Brucella melitensis* 16M at 10-fold serial diluted concentrations with detection range of $0.1\mu g mL^{-1}$ to $0.01\mu g mL^{-1}$ on 4-MBA, ZnONPs/AuNPs and ZnONPs/AuNPs/4-MBA modified SPR Au-transducer respectively.

outer membrane surface protein antigen (rOmp28 Ag) of *Brucella melitensis* 16M and characterized with one-dimensional SDS-PAGE for determining purified 32 kDa protein for animal immunization. Specific IgG-pAbs against rOmp28 protein antigen of *Brucella melitensis* 16M was prepared and single batch derived IgG-pAbs were purified (Figure 11). The rOmp28 IgG-pAbs were used as ligand for immobilization on modified surface of SPR Au-transducer to study interactive Ag to Ab (test analyte to ligand) binding affinity for *Brucella* detection at various SPR response angles with ten-fold serially diluted rOmp28 protein Ag. Detection range of $0.1\mu g mL^{-1}$ to $0.01\mu g mL^{-1}$ was used in biosensing and observed limit of lowest antigen detection at $0.1\mu g mL^{-1}$ with each SPR cycle using three different modified surfaces of Au-transducer (Figure 15). The recorded SPR response angle change at each concentration-dependent interactive binding with each modified Au-transducer surface

[on time scale above SPR angle ($m^{\circ}=20$) against each concentration] was plotted using standard graph plots respectively. This study aimed to represent modifications in SPR Au-transducer for the development of potential biosensor using combination of metal oxide nanomaterials having strong covalent binding to detect specific antigen derived antibody of *Brucella*. The study reported preliminary work on modification of SPR Au-transducer with metal oxide nanomaterials in combination using SAMs for enhanced detection of *Brucella* antigen upto femtograms level in early cases of low disease burden.

Chemical Reagents

Zinc Nitrate Hexahydrate [$Zn(NO_3)_2 \cdot 6H_2O$ Qualikems], Hexamethylenetetramine (Hexamine $C_6H_{12}N_4$ Sigma-Aldrich), Trisodium Citrate Dihydrate (Hi-media), Chloroauric Acid Trihydrate ($HAuCl_4 \cdot 3H_2O$) Sigma-Aldrich, Citric Acid Monohydrate (Sigma), Methanol (Sigma-Aldrich), Ethanol (Sigma-Aldrich), N-(3-Dimethylaminopropyl)-N'-ethylcarbodiimide Hydrochloride (EDC Sigma), N-Hydroxysuccinimide (NHS Sigma), Milli-Q Water (Milli-Q Direct 8, Millipore), 4-Methoxybenzoic Acid (4-MBA Sigma-Aldrich), Ethanolamine (Fluka Sigma), Hydrochloric Acid (0.01M HCl Fluka Sigma), Sodium Azide (Sigma-Aldrich), *Brucella* Selective Broth (BSB) Hi-media, Brain Heart Infusion Broth (BHI) and Luria Bertani Broth (LB) Hi-media, Protein-A Antibody Purification Kit (Montage-Millipore USA), Polyclonal rabbit anti-mice immunoglobulins/HRP conjugates (Dako Denmark), Isopropyl β -D-1-thiogalactopyranoside (IPTG Sigma), Urea (Sigma), Buffer Phosphate Saline (PBS, 10mM L^{-1}), Formaldehyde (Merck), Glycerol (Sigma), Complete and Incomplete Freund's Adjuvant (CFA, IFA Sigma), Phenylmethanesulfonyl Fluoride (PMSF-Sigma), Acrylamide and N,N'-Methylenebisacrylamide Sigma-Aldrich, Ammonium persulfate (Sigma-Aldrich), Sodium dodecyl sulfate ACS reagent (Sigma), Trizma base (Sigma), β -Mercaptoethanol (Merck Millipore), Bromophenol Blue (Merck), Glycine (Sigma-Aldrich), Glacial Acetic Acid (Qualigens Thermo Fisher Scientific), Coomassie Brilliant Blue R 250 (Hi-media).

Preparation of Zinc and Gold Nanomaterials (ZnONPs and AuNPs)

For ZnO nanomaterial synthesis, conventional 'Hydrothermal Method' as a chemical synthesis technique was used as explained by Chang *et al* with slight modifications [33]. To prepare zinc nanomaterial, 0.38 gm of Zinc Nitrate Hexahydrate was dissolved in 25mL of deionized water (DI) water and mixed properly to obtain a homogenous solution. Also, in another 25mL of DI water, 0.17gm of Hexamine solution was prepared by gentle mixing. These two solutions are further mixed together in a sterile glass beaker and a glass slide of standard size was placed inside the set-up beaker. Very carefully, quartz glass substrates (SPR Au-transducer chips as shown in (Figure 2) for growing ZnO seed layers were placed over the glass slides and this whole set-up was placed in another double-sized beaker with boiling water over the magnetic hot plate for continuous heating (Figure

1). The temperature of the inner beaker with 1:1 solution of zinc precursor and hexamine was maintained always between 85 to 90°C throughout the experiment for obtaining appropriate ZnO seed growth. The time duration for required growth of zinc seeds was optimized for about 4 to 5 hours with controlled temperature in dust-free sterile environment. Once, the seeds were fully grown over the substrates, they were placed on sterile petri-dishes and washed twice to thrice with DI water to remove extra material settled (if any). After drying at room temperature, substrates were annealed to enhance the crystal-

linity at 150°C for 60 minutes inside the thermal annealing oven (REMI Dry Heat Oven) and further used in the experiments. The dry powder obtained from these glass slides was used separately for nanomaterial characteristic analysis. For AuNPs preparation, standard 'Turkevich Method' using Gold Tetrachloride Trihydrate ($HAuCl_4 \cdot 3H_2O$) precursor with slight modifications was performed [34,35]. For NPs synthesis, autoclaved (121°C for 20 minutes at 15 lbs pressure using Sanyo Labo Autoclave MLS-3780) sterile glasswares after complete hot-drying (at 50 to 60°C using Labcon FSIM Incubator) were used. To prepare AuNPs, twenty mL of 1.0 mM Chloroauric Acid Trihydrate solution was freshly prepared and heated to boil (10 to 15 minutes) in sterile 50 mL glass beaker on magnetic hot plate (Spinot Magnetic Stirrer, Tarsons) with continuous stirring. In this boiling solution, 2 mL of 1 % freshly prepared Trisodium Citrate Dihydrate solution was added slowly with continuous vigorous stirring (Figure 1). During the gold reduction process, colour of solution changes from pale yellow to colourless and finally a violet to deep red violet colour was inferred. After continuous boiling for 15 to 20 minutes, solution was cooled at Room Temperature (RT) and its pH was measured. The citrate synthesis using $HAuCl_4 \cdot 3H_2O$ resulted in capped 'Gold-Sol Colloid' with process modification in citrate buffer where a homogeneous mixture of 75% to 80% citrate and 25% to 30% citric acid was preferably used for reduction. The prepared AuNPs were further precipitated by centrifugation at high speed (30 minutes at 15,000 rpm) and vacuum dried (Jouan RC 10.22, Thermo Fisher Scientific) for 6 to 7 hours for their characteristic physico-chemical analysis.

Characterization of Synthesized Nanomaterials (ZnONPs and AuNPs)

The synthesized Zn and Au nanomaterials for Ag-Ab based surface interaction study were characterized for their physico-chemical properties by using UV-Visible Spectroscopy (Shimadzu UV-2450), SEM-EDX (HR FESEM with EDX, ULTRA Plus Model) and TEM (JEOL 1230) analysis SAED for size, shape and chemical structure analysis, FT-IR (Perkin Elmer, Model Spectrum Two) for elemental composition with functional group analysis and, Powder-XRD (RIGAKU, Mini Flex 600, 5th Generation with Cu-K α 1 radiation) for analysis of chemical nature and stoichiometric surface morphology.

Bacterial Culture Growth Conditions and Standard Strains Used for the Study

In this comparative study with sensor based surface-mediated antigen and antibody interactions, *Brucella melitensis* 16M (NCTC 10094) gram-negative alphaproteobacteria as standard strain of genus *Brucella* obtained from National Collection of Type Cultures (NCTC), Public Health England (PHE, UK) along with its *Escherichia Coli* (BL-21) derived recombinant rOmp28 positive clone established in our laboratory were used [36]. Both the cultures were preserved and routinely maintained in 30% glycerol with their ambient storage at -80°C. For obtaining fresh bacterial culture, they were grown in supplemented BSB and LB growth media's at 37°C incubation inside the gyrating shaker incubator (Labcon 5081U shaking incubator, USA) maintained at a continuous constant shaking speed of 180 rpm respectively. The recombinant BL-21 positive clone culture was grown with 50 μ g mL^{-1} kanamycin sulphate antibiotic supplement selection. These cultures were handled and maintained in the High Containment Facility of our laboratory (HCF at DRDE-DRDO, Gwalior, India) by following all standard operating procedures and necessary methods.

Brucella Specific Recombinant rOmp28 Protein Expression and Purification

The recombinant outer membrane rOmp28 protein used in this study was expressed and purified from its *Escherichia coli* BL-21 positive clone obtained by bacterial molecular cloning already established in our laboratory [36,37]. The positive clone was derived from *Escherichia coli* BL-21 expression host which was transformed earlier with pET-28a (+) plasmid and ligated with selective *Omp28* (753bp) gene fragment of *Brucella melitensis* 16M. For expression and purification of rOmp28 protein for SPR biosensor study, its PCR confirmed clone with amplified gene was grown and induced with 1 mM IPTG for 5 hours at 37°C incubation at rotation speed of 180 rpm inside the gyrating shaker incubator. The induced grown culture was further lysed under denaturing conditions in Urea and purified with His-tag binding Ni-NTA gel filtration (Ni-NTA Gel Superflow, Qiagen) affinity column chromatography using different pH-gradient buffers [Lysis (pH-8.0), Wash (pH-6.3) and Elution (pH-4.3) Buffers] as mention by Thavaselvam D *et al.* Purified rOmp28 protein was dialysed and de-salted with Urea buffer from higher to lower molar concentration changes (6M, 4M and 2M Urea) followed by 1XPBS (pH 7.2) standard saline buffer change and obtained protein was estimated for characteristic analysis with Folin-Lowry and SDS-PAGE gel electrophoresis respectively [38,39].

Recombinant rOmp28 Derived IgG-pAbs Production for Affinity Purification

Two groups of female BALB/c mice with six mice in each group were immunized with PBS suspended purified rOmp28 protein Ag for production of specific IgG-pAbs. Five mice were subjected for scheduled immunization and sixth as experiment control for pre-immune sera (PIS, Negative Sera) collection. For immunization doses, 50 µg of purified rOmp28 Ag was administered at an interval of 1 week over a period of 2 months with total six booster doses (Day 0) - pooled PIS sera was collected, (Day 7) - rOmp28 protein antigen priming with Complete Freund's Adjuvant (CFA) and (Day 14 to 49) - subsequent booster doses with Incomplete Freund's Adjuvant (IFA) [40]. The titer of antibody was estimated with standardized I-ELISA against immobilized rOmp28 antigen on ELISA modules. For purification of IgG-pAbs, whole blood collected from immunized animals was pooled and incubated at 37°C for complete 1 hour and centrifuged at 5,000 rpm for 10 minutes at 4 °C to obtain the polyclonal antibody rich Hyper Immune Sera (HIS) supernatant. The supernatant was then subjected for affinity column purification with Montage protein-A (Montage-Millipore, USA) antibody purification kit following the manual instructions. The estimated IgG antibody was stored at -20°C using sodium azide for active preservation until further use. Single batch polyclonals were purified from two experimental groups in order to avoid antibody batch-to-batch variations. Purified IgG polyclonals were characterized using SDS-PAGE and Immunoblot analysis for determining immuno-reactive sensitivity and purity of the purified test protein. Further, for the estimation of HIS antibody titers, 20 µg mL⁻¹ of rOmp28 protein as coating antigen in 0.05M carbonate-bicarbonate buffer (pH 9.6) was immobilized on ELISA immunomodules (Thermo-Nunc F8 Loose Maxisorp Modules). The modules were immobilized with Ag for overnight incubation (O/N at 4°C). Washed with PBS/PBS-T thrice and blocked with 2 % BSA (O/N at 4°C). The ELISA and SDS-PAGE with characteristic Western blot was performed as per the protocol mentioned by Hans R *et al* 2020 [41]. Six mg mL⁻¹ of purified IgG-pAbs was obtained

using standard Folin Lowry's protein estimation and was stored at -20°C till further use for SPR biosensing.

SPR Biosensor Study for Brucella Detection with Immobilized rOmp28-IgG pAbs

For SPR biosensor based biodetection of *Brucella melitensis* 16M, purified rOmp28 mice IgG pAbs (ligand as detection antibody) were immobilized on the surface of modified Au-transducer as explained by Hans R *et al* 2020 in order to study the relative trend in Ag-Ab biomolecular surface interactions.

Modification of SPR Gold-Chip/Au-transducer with 4-MBA

Experimental methodology for biosensing and surface modification of SPR Au-transducer with 0.01 M methanolic solution of 4-MBA was performed as explained by Sikarwar B *et al* 2017 [42]. Au-transducer chips were completely washed with methanol and 4-MBA methanolic solution was spin coated over the surface of Au-chips followed by complete drying at a rotational speed of 2500rpm for 20 minutes. For SPR bio-sensing, three step automated process with association (500s), dissociation (400s), and transducer surface regeneration (120s) followed by automated injection of analyte (75 µL by volume) was performed (Figure 12). A double channel SPR system having 384 microplate wells were used for sample acquisition in each cycle of biosensing process and the test samples (analyte and ligand) were mixed at flow rate speed of 16.7µL s⁻¹. Sterile-filtered phosphate buffer saline (pH 7.2) was used as washing buffer (running buffer) in each SPR cycle for maintaining the structural stability of tested proteins. For obtaining interaction curve values of SPR binding, *Brucella melitensis* rOmp28 IgG-pAbs were immobilized on the various modified surfaces of SPR-transducer and allowed to interact with rOmp28 protein antigen of *Brucella melitensis* 16M at different ten-fold serial dilution concentrations (0.1µg mL⁻¹ to 0.01fg mL⁻¹) respectively. The concentration based SPR binding curve values of association were plotted using standard graph plots to analyse the effect of different surface modifications of biosensor for *Brucella* detection.

Modification of SPR Au-transducer with ZnONPs and AuNPs

For SPR transducer modification with synthesized ZnO nanomaterial along with AuNPs, the SPR Au-chips were properly cleaned with fresh methanol and dried over the spin coater at a rotation speed of 100 rpm for 5 minutes. Seventy Five µL of Zinc Nitrate solution was gently dispersed at the centre of chip rotating at continuous speed of 100rpm. For complete drying, chips were initially rotated at 300rpm for 5 minutes followed by 2500rpm for another 10 to 15 minutes in a closed sterile environment and subjected to hydrothermal synthesis of nanomaterials on quartz chips. In order to further modify ZnONPs coated SPR chip surface with AuNPs, coated chips were used for the photo-catalytic UV deposition of gold. In this process, 0.1 mM fresh aqueous solution of Gold Tetrachloride Trihydrate (HAuCl₄.3H₂O) was prepared in DI water for AuNPs synthesis as mentioned above and ZnONPs modified SPR chips were completely immersed in sterile glass petri-plates containing the prepared gold nanoparticles sol-colloid. The set-up was kept in continuous UV light for about 20 minutes and slowly rinsed with sterile DI water for further drying by thermal annealing at 50°C temperature. These prepared Au-transducers with ZnONPs and AuNPs based surface modification were later used in SPR-biosensing experiments.

Modification of Au-transducer with ZnONPs, AuNPs and 4-MBA

In another type of SPR transducer surface modification, first of all seeded ZnO SPR transducer chips (see ZnO nanomaterial preparation) were coated with AuNPs sol-colloid prepared using Turkevich method through photo-catalytic UV deposition method (as above). Over the surface of these AuNPs deposited chips, again 75 μ L of freshly prepared 0.01M methanolic solution of 4-MBA was spin-coated and dried as above mentioned. As a result, a three-layered modified SPR Au-transducer surface with ZnONPs/AuNPs/4-MBA was obtained respectively.

Immobilization of *Brucella melitensis* 16M rOmp28 IgG-pAbs on Transducer Surface

For SPR surface-binding experiments, affinity purified rOmp28 mice IgG-pAbs were immobilized on the surface of various modified Au-transducers (as explained by Hans R *et al*) to analyse the surface-mediated Ag-Ab biomolecular interactions and relative trends in concentration-dependent analyte to ligand binding affinity. During the experiment, SPR chip was washed at every 120 s interval for 600 s with continuous 50 μ L of running buffer to obtain a constant SPR baseline from dual SPR channels prior to IgG-pAbs immobilization. Seventy five μ L of EDC and NHS solution was injected for activation of the coated surface and 75 μ L of ethanolamine was also added for blocking the non-specific binding sites and non-reacted NHS ester groups (Figure 12). After each SPR interaction cycle, transducer surface was regenerated by passing HCl solution in dual channels (experiment and reference channels). With each cycle, SPR binding interaction values according to varying concentration of the analyte was recorded and standard graphs were plotted for analysis of these modified surface-mediated interactions.

Results and Discussion

Preparation of ZnO Nanomaterial and AuNPs

Hydrothermal preparation of ZnO nanomaterials at a constant high temperature of 90 $^{\circ}$ C with latent annealing at temperature 150 $^{\circ}$ C resulted in pure crystalline hexagonal wurtzite nanostructure in between 100nm to 200nm particle size (Figure 4). Its polycrystalline nature was also determined by the appearance of regular concentric bright rings in TEM-SAED patterns with d-spacing value almost identical with XRD patterns (Figure 4, 5, 6 and 7). The nature of ZnO seed growth was found typically anisotropic as a favoured growth in high ionic strength of DI water and hexamine. However, gold nanoparticles prepared from Turkevich Method were observed as spherical in shape with crystalline structure. On reduction of metallic gold from Au³⁺ to Au⁰ at 0.1mM of precursor concentration, they appeared as stable mono-dispersed round-sphere like colloid particles of diameter analysed with TEM in between 50 to 100 nm as shown in (Figure 4 and 6).

UV-Visible Analysis of Nanomaterials

Characterization of nanomaterials with UV-Vis analysis recorded absorbance of the samples displaying absorption spectra peak at λ_{max} value of 370nm and 520nm for ZnONPs and AuNPs respectively as near to reported value (Figure 3). The sharp rise and increase in the optical absorption spectra determine gradual growth of particle size in single phase with fewer eccentricities for Au nanomaterial and hexagonal wurtzite anisotropic crystalline growth for ZnO nanomaterial respectively.

Characterization Using SEM-EDX and TEM-SAED Microscopy

On analysing the samples for SEM-EDX, hexagonal blob

shaped nanostructures of ZnO were observed with anisotropic growth patterns of EDX spectrum showing pure atomic percentage of its elemental composition on Au-transducer surface (See Figure 4a, 5a and supplementary data). ZnO surface stoichiometry elemental composition was attributed at 1:2 atomic ratios on SEM analysis. SEM with Au nanomaterial displayed spherical shaped Au nanoparticles with uniform and identical particle size having pure gold EDX spectrum (100 % atomic element composition) (see Figure 4b, 5b and supplementary data). No suspended particle aggregation was observed further with TEM analysis of the nanomaterials (as shown in Figure 6). For characterization with TEM, copper mesh grid with a test sample drop having mixture of sample and isopropanol were analysed at 120kV. For ZnO nanomaterial, nano-metallic particle size in range of 100 to 200nm diameter was observed with TEM and SAED patterns of bright sharp spots on concentric rings indicating polycrystalline nature with symmetrical orientation of ZnO (Figure 6a, b, c and 7a). For Au nanomaterials, TEM analysis revealed round sphere like particles in range of 50 to 100 nm with SAED patterns of concentric bright spots corresponding to polycrystalline nature of particles (Figure 6d, e, f and 7b).

Powder-XRD and FT-IR Chemical Analysis

For characteristic chemical structure and composition, XRD analysis was performed for both ZnO and Au nanomaterials (see Figure 9 and supplementary data). The diffraction studies for ZnO nanomaterial displayed characteristic diffraction peaks with 2θ values at 31.84 $^{\circ}$, 34.52 $^{\circ}$, 36.33 $^{\circ}$ and 47.63 $^{\circ}$ for corresponding reflections of (100), (002), (101) and (102) set of planes in a face centered cubic (fcc) lattice of cubic crystal system. And, indexed as hexagonal wurtzite phase of ZnO along with an extra peak of 38.1 $^{\circ}$ for gold transducer surface where the ZnO seed growth was monitored for direct XRD analysis (as shown in Figure 9a). And, characteristic diffraction peaks for AuNPs were observed with 2θ values at 38.16 $^{\circ}$, 44.31 $^{\circ}$, 64.41 $^{\circ}$ and 77.50 $^{\circ}$ for corresponding reflections of (111), (200), (220) and (311) set of planes in a Face Centered Cubic (fcc) lattice of crystal system (as shown in Figure 9b). Along with chemical nature and structure prediction, the frequency based vibrational and absorption appearance for corresponding functional groups was also analysed using FT-IR (wave number range of 4,000 cm^{-1} to 500 cm^{-1}) analysis (Figure 8). For ZnO, absorption at 3,500 to 3,450 cm^{-1} corresponds to N-H stretching vibrations of primary amines along with medium O-H stretching of intermolecular bonding, sharp strong broad peaks at 1,550 to 1,500 cm^{-1} ascribed to N-O stretchings of nitro functional group, another strong absorption peak at 1,342 to 1,266 cm^{-1} and 1,250 to 1,020 cm^{-1} originated from C-N stretching vibration of amines and aromatic amines. The medium strength peaks appeared at 1,395 to 1,310 cm^{-1} was assigned to O-H bending vibrations of pendant carboxylic groups and strong peaks observed at 995 to 985 cm^{-1} originated from monosubstituted C=C alkenes bending by frequency as shown in FT-IR spectrum 'b' of Figure 8 and supplementary data. Similarly, for AuNPs, absorption at 3,400 to 3,300 cm^{-1} corresponds to medium N-H stretching vibrations of hydrogen bonds in amines along with strong peaks of pendant hydroxyl groups. The sharp and broad peaks at 3,300 to 2,500 cm^{-1} indicated O-H stretching of carboxylic and weak S-H stretchings of thiol groups. Another absorption peaks observed at 1,640 to 1,403 cm^{-1} relates to strong C=O stretching vibrations of amides, C=C stretching of monosubstituted alkenes along with pendant carboxylic groups. The strong C-H stretching vibrations appeared at peak 2,983 cm^{-1} of $-\text{CH}_2$ group corresponds to reduction of gold and a shift of absorption peaks at 2,600 to

2,550 cm^{-1} , 1,643 cm^{-1} and 1,275 to 1,250 attributed to weak S-H stretching, strong C=C vibrations and medium C-O stretching's with O-H bending vibration of thiol, mono-substituted alkenes and alky aryl functional groups respectively (see FT-IR spectrum 'a' of Figure 8). Other absorption peaks at frequency 1,505 cm^{-1} , 1,382 cm^{-1} , 1,085 cm^{-1} and 1,044 cm^{-1} corresponds to relative stretching vibrations of N-O for nitro group, C-H bending and C-O stretching of alkanes and alcohols respectively.

One-Dimensional SDS-PAGE Gel Electrophoresis

For gel electrophoresis analysis, SDS-PAGE with 12% gel composition with 5 μL of lysed sample was run on BIO-RAD Mini-PROTEAN Tetra Cell unit and a 32 kDa purified rOmp28 protein antigen of *Brucella* was analysed for further use in production of mice IgG-pAbs for SPR bio sensing study (Figure 11a). Total 3 to 6mg mL^{-1} (batch-to-batch) of protein was estimated and 50 $\mu\text{g mL}^{-1}$ of dialysed rOmp28 protein Ag was administered in two experimental animal groups for the production of specific rOmp28 IgG-pAbs. Similarly, after purification, IgG-pAbs were analysed with I-ELISA for antibody titer estimation as mention by Hans *et al* and was estimated $\geq 64,000$ dilutions compared to PIS control (Figure 10). On analysis with SDS-PAGE, 5 μL lysed sample resulted in two fragments corresponding to heavy (50 kDa) and light (25 kDa) chain of pAbs (Figure 11c).

Western Blot Characterization for Specificity of rOmp28 IgG-pAbs

Purified rOmp28 protein Ag analysed with SDS-PAGE was subjected for immunoblot analysis and transferred to nitrocellulose membrane for determining characteristic immuno-reactivity with polyclonals. IgG-pAbs at 1:100 dilution suspended in 1X PBS buffer resulted in strong positive blot of 32 kDa protein showing specific immuno-reactivity and affinity towards rOmp28 recombinant protein (Figure 11a and b). Immunoblot results attributed to its potential application for further immobilization on SPR Au-transducer surface as ligand and specific detection antibody to capture *Brucella* surface Ags.

Immobilization of rOmp28 IgG-pAbs on SPR-Au Transducer Surface

The active immobilization of detection antibody rOmp28 IgG-pAbs on the surface of modified Au-transducer depends on the pH of buffer in which the antibody was concentrated on the surface. Here for SPR bio-sensing, sterile 1X PBS (10mM L^{-1} at pH 7.2) was used for antibody pre-concentrations which was kept below the protein isoelectric point like for pAbs PI at 9, such that suitable pH gradient can be established between sensor surface and ligand for accurate immobilization on the modified SPR biosensor (Figure 12). The pH on activation of SPR channel with EDC/NHS results in pH higher than 3.5 on the surface and EDC requires uncharged amine groups for interaction. Therefore, neutral pH of ligand facilitates noise free signals on surface immobilization as explained by Hans *et al* 2020. The SPR sensogram included a complete nine major steps for ligand immobilization on transducer surface as shown in Figure 12 respectively. The immobilized mice IgG-pAbs on interaction with characteristic analyte rOmp28 Ag of *Brucella melitensis* 16M reflected change in SPR angle response as shown in SPR sensogram with ZnONPs (see Figure 13 and supplementary data) alone and with ZnONPs/AuNPs layered combination during process optimization and was collectively plotted with standard graphs as shown in Figure 13, 14 and 15. Therefore, during surface interaction study as observed with relative change in SPR response angles

(m°) detection antibody was found sensitive in bio-sensing different 10 fold serial concentrations of rOmp28 Ag (0.1 $\mu\text{g mL}^{-1}$ to 0.1fg mL^{-1}) for all three modified Au-transducer surfaces viz; 4-MBA, ZnO/AuNPs and ZnO/AuNPs/4-MBA respectively.

Surface Interaction Binding Study with Various SPR Au-transducer Modifications

For SPR biosensing, immobilized rOmp28 IgG-pAbs was allowed to interact in concentration-dependent manner with 10-fold serial diluted concentrations of rOmp28 antigen (0.1 $\mu\text{g mL}^{-1}$ to 0.1fg mL^{-1}) of *Brucella melitensis* 16M. The active and specific interaction between analyte and ligand resulted in lowest Limit Of Detection (LOD) at 0.1fg mL^{-1} with ZnONPs/AuNPs and ZnONPs/AuNPs/4-MBA (Figure 15b and c). On comparing SPR surface response with applied three different modifications on Au-transducer, it was analysed that on Ag-Ab interactions during SPR biosensing with initial concentration of 0.1 $\mu\text{g mL}^{-1}$ of rOmp28 Ag followed by its 10 fold serial detection, sensitivity towards antigen detection was obtained in the order; 4MBA (at 83.7 $^\circ$) < ZnONPs/AuNPs (at 98.9 $^\circ$) < ZnONPs/AuNPs/4-MBA with SPR response angle at 179.2 $^\circ$ respectively (Figure 15). And, LOD for the interactive study was analysed as 4-MBA at 0.01pg mL^{-1} lesser than the Au-transducer surface modified with ZnONPs/AuNPs and ZnONPs/AuNPs/4-MBA at 0.1fg mL^{-1} respectively (as shown in Figure 15a, b and c). For determining relative increase in SPR response angle change during Ag-Ab interactions in association cycle, 4-MBA and ZnONPs/AuNPs modified surface resulted in less response as compared to the ZnONPs/AuNPs/4-MBA modified transducer surface. On comparison, ZnONPs/AuNPs/4-MBA modification was found efficient in *Brucella* antigen detection with increased sensitivity relative to total SPR response angle change in concentration-dependent biomolecular interaction. Therefore, evaluated potential combination of ZnONPs/AuNPs/4-MBA for biosensor surface modification can be considered as, highly sensitive, fast, label free specific biosensor and a real-time platform for on-field antibody-based detection of *Brucella*.

Conclusion

Brucella is occupied by multiple disease presentations and often mis-diagnosed with other differential disease pathogens. Its febrile illness is not much fatal but imposes serious disease burdens on achieving successive chronicity within the diverse groups of population world-wide. Suggestions and implications in established diagnostic methods for specific detection is challenging but when used in combination with gold standards present existing disease pathogenicity and new potential hot-spots. The serological tests which are used in most of the preliminary detection are based on the detection of circulating antibodies developed against surface antigens of *Brucella*. In our present study, we have explored the potential efficacy of such polyclonal antibodies in targeting sensitive and specific detection of *Brucella*. We have evaluated in our study that a 28 kDa outer membrane protein of *Brucella* is a suitable alternate to Lipopolysaccharide LPS-based surface Ag detection as they offer more specificity and are localized having no relative homology with other related bacterial species. Therefore, we cloned, expressed and purified 28 kDa (Omp28) surface protein of *Brucella melitensis* 16M in *Escherichia coli* (BL-21) expression host and obtained a recombinant rOmp28 (32 kDa) outer membrane protein antigen of *Brucella*. It was well characterized using indirect ELISA in our laboratory and further reported for its detection potential in clinical diagnosis. In this study, we have used this recombinant antigen to develop specific IgG-pAbs sensitive for

detection of *Brucella melitensis* 16M. These antibodies raised in BALB/c mice were affinity purified and immobilized on the surface of SPR Au-transducer with enhanced modifications using Zn and Au nanomaterials. Since, the antibodies are considered as multivariate and possess efficient capture affinity with multiple surface orientations towards the localized epitopes of antigens. This potential ability of covalent affinity for antigen is explored whereby, we have modified SPR Au-transducer surface to increase the number of active sites for amine coupling with the ligand antibodies. Moreover, these numbers of active binding sites also increases with layered NPs to establish more antibody covalent bindings during sensor activation using EDC/NHS. This activation brings more and more thiol and carboxylic acid rich entities to increase SPR response angle during effective and specific Ag to Ab interactions. Further, the functionalized NPs with EDC/NHS activation and selective antibody loadings improve biosensing due to their remarkable optical properties and increased amide linkages. When concentration-dependent detection was analysed it was observed that the SPR response angle gradually increase with net SPR effect with modified surfaces using combination of nanomaterials. Therefore, our findings conclude that biosensor modification with metal oxides nano-hybrids (ZnONPs/AuNPs/4-MBA) or nanoconstructs in association with chemical probes can facilitate increased ratio of antigen to antibody (rOmp28 Ag to IgG-pAbs) for affinity binding in surface based interaction studies. In this leading-edge-strategy of layering ZnONPs and AuNPs, hexagonal close packing of ZnONPs Wurtzites is having Zn²⁺ ions in tetrahedral holes occupying spherical AuNPs and distributes an array of its lattice sites for amino acid coupling in conjunction with EDC/NHS activation for enhanced peptide coupling with carboxylic-terminated colloidal AuNPs. Moreover, such overlapping and layering of NPs on biosensors can be used to detect minimum number of *Brucella* antigens available in chronic disease cases where the infection persist intracellularly inhabiting host immune macrophages. The increased density of selective antibodies on the surface of NPs mimics biological bacterial cell with multiple antigenic sites and thus responds in maximum capture of specific *Brucella* surface antigens. The neutral pH of buffer where Ag to Ab covalent binding occur maintains controlled orientation to increase the net surface coverage with stable structure of interactive protein moieties. Modification of biosensor surface with NPs and SAMs like chemical probes itself contributes towards the maximum adsorption of such interactive species. Thus, modification of biosensors with combinations of NPs enhances potential antibody avidity and affinity towards the interactive antigens. SPR biosensor are portable and can be deployed in field studies with reduced detection time in about few minutes and when modified or fabricated with nanostructures having specific immobilized antibodies provide accurate, fast and reproducible results with invariable specificity and sensitivity for early disease diagnostics.

Supporting Information

Supplementary data set is available as mentioned in the text.

Ethical Approval

The following research work was carried out at Defence Research and Development Establishment (DRDE-DRDO), Ministry of Defence, Government of India and approved by the Institutional Animal Ethics Committee (No: 37/GO/Rbi/S/99/CPCSEA and IAEC MB-43/57/DTS Dated: 14/06/2018 and IAEC BDTE-01/59/SP Dated: 05/06/2020) for the purpose of control and supervision of experimental animals. All methods performed

in the study were executed and completed in accordance with the proper guidelines and ethical regulations. This study was also approved by Institutional Biosafety Committee of the Defence Research and Development Establishment (DRDE-DRDO), Ministry of Defence, Government of India vide protocol no. IBSC/15/MB/DTS/6.

Author Contributions

D.T. and R.H. have designed the experiments. R.H. has performed all the experiments, characteristic analysis and manuscript writing. D.T. and R.H. have evaluated and analysed the experimental results. D.T. has accepted, reviewed and revised the complete manuscript. This research work was completed by R.H. under the proper guidance of D.T.

Conflict of Interest

The authors declare no competing conflicts of interest.

Acknowledgement

The authors are thankful to Dr. Manmohan Parida, Director, Defence Research and Development Establishment, Defence Research and Development Organisation (DRDO), Jhansi Road, Gwalior - 474002 (M.P.), India, for his encouragement and continuous support for this study. Also, the authors extend their acknowledgements to faculty of Dr. A.P.J. Abdul Kalam, Central Instrumentation Facility (C.I.F.), Jiwaji University, Gwalior and Indian Institute of Science Education and Research (IISER), Bhopal, India, for providing necessary instrumentation for this study.

References

- O'Callaghan D. Human Brucellosis: Recent Advances and Future Challenges. *Infect Dis Poverty*. 2020; 9: 101.
- Godfroid J, Al Dahouk S, Pappas G, Roth F, Matope G, Muma J, et al. A "One Health" Surveillance and Control of Brucellosis in Developing Countries: Moving Away from Improvisation. *Comp Immunol Microbiol Infect Dis*. 2013; 36: 241-248.
- Lim ML, Rickman, LS. Brucellosis, *Infect Dis Clin Pract (Baltim Md)*. 2004; 12: 7-14.
- Nagalingam M, Shome R, Balamurugan V, Shome BR, Narayana RK, Vivekananda IS, et al. Molecular Typing of *Brucella* Species Isolates from Livestock and Human. *Trop Anim Health Prod*. 2012; 44: 5-9.
- De Massis F, Zilli K, Di Donato G, Nuvoloni R, Pelini S, Sacchini L, et al. Distribution of *Brucella* Field Strains Isolated from Livestock, Wildlife Populations, and Humans in Italy from 2007 to 2015. *PloS One*. 2019; 14: e0213689.
- Gong QL, Sun YH, Yang Y, Zhao B, Wang Q, Li JM, et al. Global Comprehensive Literature Review and Meta-Analysis of *Brucella* spp. in Swine Based on Publications from 2000 to 2020. *Front Vet Sci*. 2021; 8: 630960.
- Matle I, Ledwaba B, Madiba K, Makhado L, Jambwa K, Ntushelo N. Characterisation of *Brucella* Species and Biovars in South Africa Between 2008 and 2018 using Laboratory Diagnostic Data. *Vet Med Sci*. 2021; 7: 1245-1253.
- Shakir R. Brucellosis. *J Neurol Sci*. 2021; 420: 117280.
- Migisha R, Dan N, Boum Y, Page AL, Zuniga-Ripa A, Conde-Alvarez R, et al. Prevalence and Risk Factors of Brucellosis Among Fertile Patients Attending a Community Hospital in South Western Uganda. *Sci Rep*. 2018; 8: 15465.
- Peng H, Bilal M, Iqbal H. Improved Biosafety and Biosecurity Measures and/or Strategies to Tackle Laboratory-Acquired In-

- fections and Related Risks. *Int J Environ Res Public Health*. 2018; 15: 2697.
11. The World Bank. *World Livestock Disease Atlas: A Quantitative Analysis of Global Animal Health Data (2006-2009)*. World Bank, Washington, DC, 2011.
 12. Bodenham RF, Lukumbagire AS, Ashford RT, Buza JJ, Cash-Goldwasser S, Crump JA, et al. Prevalence and Speciation of Brucellosis in Febrile Patients from a Pastoralist Community of Tanzania. *Sci Rep*. 2020; 10: 7081.
 13. Mangalgi S, Sajjan A. Comparison of Three Blood Culture Techniques in the Diagnosis of Human Brucellosis. *J Lab Physicians*. 2014; 6: 14-17.
 14. Buzgan T, Karsen H, Karahocagil MK, Akdeniz H, Sunnetcioglu M. A Case of Brucellosis Presenting as High Titer Negative Result by Standard Tube Agglutination Test. *Mikrobiyol Bul*. 2007; 41: 151-154.
 15. Shemesh AA, Yagupsky P. Limitations of the Standard Agglutination Test for Detecting Patients with *Brucella melitensis* Bacteremia. *Vector Borne and Zoonotic Dis*. 2011; 11: 1599-1601.
 16. Zeytinoglu A, Turhan A, Altuglu I, Bilgic A, Abdoel TH, Smits HL. Comparison of *Brucella* Immunoglobulin M and G Flow Assays with Serum Agglutination and 2-Mercaptoethanol Tests in the Diagnosis of Brucellosis. *Clin Chem Lab Med*. 2006; 44: 180-184.
 17. Bastos CR, Mathias LA, Jusi M, Santos R, Silva G, Andre MR, et al. Evaluation of Dot-Blot Test for Serological Diagnosis of Bovine Brucellosis. *Braz J Microbiol*. 2018; 49: 564-568.
 18. Hajia M, Fallah F, Angoti G, Karimi A, Rahbar M, Gachkar L, et al. Comparison of Methods for Diagnosing Brucellosis. *Lab Med*. 2013; 44: 29-33.
 19. Kalleshmurthy T, Skariah S, Rathore Y, Ramanjinappa KD, Nagaraj C, Shome BR, et al. Comparative Evaluation of Fluorescence Polarization Assay and Competitive ELISA for the Diagnosis of Bovine Brucellosis Vis-a-Vis Sero-Monitoring. *J Microbiol Methods*. 2020; 170: 105858.
 20. Al Dahouk S, Tomaso H, Nockler K, Neubauer H, Frangoulidis D. Laboratory-Based Diagnosis of Brucellosis - A Review of the Literature. Part II: Serological Tests for Brucellosis. *Clin Lab*. 2003; 49: 577-589.
 21. Vatankhah M, Beheshti N, Mirkalantari S, Khoramabadi N, Aghababa H, Mahdavi M. Recombinant Omp2b Antigen-Based ELISA is an Efficient Tool for Specific Serodiagnosis of Animal Brucellosis. *Braz J Microbiol*. 2019; 50: 979-984.
 22. De Klerk E, Anderson R. Comparative Evaluation of the Enzyme-Linked Immunosorbent Assay in the Laboratory Diagnosis of Brucellosis. *J Clin Microbiol*. 1985; 21: 381-386.
 23. Dal T, Kara SS, Cikman A, Balkan CE, Acikgoz ZC, Zeybek H, et al. Comparison of Multiplex Real-Time Polymerase Chain Reaction with Serological Tests and Culture for Diagnosing Human Brucellosis. *J Infect Public Health*. 2019; 12: 337-342.
 24. Mohseni K, Mirnejad R, Piranfar V, Mirkalantari S. A Comparative Evaluation of ELISA, PCR, and Serum Agglutination Tests for Diagnosis of *Brucella* using Human Serum. *Iran J Pathol*. 2017; 12: 371-376.
 25. Limo MJ, Sola-Rabada A, Boix E, Thota V, Westcott ZC, Puddu V, et al. Interactions Between Metal Oxides and Biomolecules: From Fundamental Understanding to Applications. *Chem Rev*. 2018; 118: 11118-11193.
 26. Eivazzadeh-Keihan R, Pashazadeh-Panahi P, Mahmoudi T, Chenab KK, Baradaran B, Hashemzaei M, et al. Dengue Virus: A Review on Advances in Detection and Trends - From Conventional Methods to Novel Biosensors. *Mikrochim Acta*. 2019; 186: 329.
 27. Li S, Liu Y, Wang Y, Wang M, Liu C, Wang Y. Rapid Detection of *Brucella* spp. and Elimination of Carryover using Multiple Cross Displacement Amplification Coupled with Nanoparticles-Based Lateral Flow Biosensor. *Front Cell Infect Microbiol*. 2019; 9: 78.
 28. Shams A, Rahimian Zarif B. Designing an Immunosensor for Detection of *Brucella abortus* Based on Coloured Silica Nanoparticles. *Artif Cells Nanomed Biotechnol*. 2019; 47: 2562-2568.
 29. Wu H, Zuo Y, Cui C, Yang W, Ma H, Wang X. Rapid Quantitative Detection of *Brucella melitensis* by a Label-Free Impedance Immunosensor Based on a Gold Nanoparticle-Modified Screen-Printed Carbon Electrode. *Sensors (Basel)*. 2013; 13: 8551-8563.
 30. Wahab R, Khan ST, Ahmad J, Musarrat J, Al-Khedhairi AA. Functionalization of Anti-*Brucella* Antibody on ZnO-NPs and Their Deposition on Aluminium Sheet Towards Developing a Sensor for the Detection of *Brucella*. *Vacuum*. 2017; 146: 592-598.
 31. Tripathy N, Kim DH. Metal Oxide Modified ZnO Nanomaterials for Biosensor Applications. *Nano Converg*. 2018; 5: 27.
 32. Raha S, Ahmaruzzaman M. ZnO Nanostructured Materials and Their Potential Applications: Progress, Challenges and Perspectives. *Nanoscale Adv*. 2022; 4: 1868-1925.
 33. Chang FM, Brahma S, Huang JH, Wu ZZ, Lo KY. Strong Correlation Between Optical Properties and Mechanism in Deficiency of Normalized Self-assembly ZnO Nanorods. *Sci Rep*. 2019; 9: 905.
 34. Turkevich J, Stevenson PC, Hillier J. A Study of the Nucleation and Growth Processes in the Synthesis of Colloidal Gold. *Discuss Faraday Soc*. 1951; 11: 55-75.
 35. Laaksonen T, Ahonen P, Johans C, Kontturi K. Stability and Electrostatics of Mercaptoundecanoic Acid-Capped Gold Nanoparticles with Varying Counterion Size. *Chemphyschem*. 2006; 7: 2143-2149.
 36. Thavaselvam D, Kumar A, Tiwari S, Mishra M, Prakash A. Cloning and Expression of the Immunoreactive *Brucella melitensis* 28kDa Outer-Membrane Protein (Omp28) Encoding Gene and Evaluation of the Potential of Omp28 For Clinical Diagnosis of Brucellosis. *J Med Microbiol*. 2010; 59: 421-428.
 37. Tiwari S, Kumar A, Thavaselvam D, Mangalgi S, Rathod V, Prakash A, et al. Development and Comparative Evaluation of a Plate Enzyme-Linked Immunosorbent Assay Based on Recombinant Outer Membrane Antigens Omp28 and Omp31 for Diagnosis of Human Brucellosis. *Clin Vaccine Immunol*. 2013; 20: 1217-1222.
 38. Lowry OH, Rosebrough NJ, Farr AL, Randall RJ. Protein Measurement with the Folin Phenol Reagent. *J Biol Chem*. 1951; 193: 265-275.
 39. Laemmli UK. Cleavage of Structural Proteins during the Assembly of the Head of Bacteriophage T4. *Nature*. 1970; 227: 680-685.
 40. Zhang Y, Bao H, Miao F, Peng Y, Shen Y, Gu W, et al. Production and Application of Polyclonal and Monoclonal Antibodies against *Spiroplasma eriocheiris*. *Sci Rep*. 2015; 5: 17871.
 41. Hans R, Yadav PK, Sharma PK, Boopathi M, Thavaselvam D. Development and Validation of Immunoassay for Whole Cell Detection of *Brucella abortus* and *Brucella melitensis*. *Sci Rep*. 2020; 10: 8543.
 42. Sikarwar B, Singh VV, Sharma PK, Kumar A, Thavaselvam D, Boopathi M, et al. DNA-Probe Target Interaction Based Detection of *Brucella melitensis* by using Plasmon Resonance. *Biosens Bioelectron*. 2017; 87: 964-969.